

# Proposed Model for Pyroelectric Effect in Poly(vinylidene Fluoride)

TARA KAURA and RABINDER NATH, *Physics Department, University of Roorkee, Roorkee-247672, India*

## Synopsis

A new model is given to account for the pyroelectric effect in poly(vinylidene fluoride). Hopping of trapped charge carriers over the potential barrier and the existence of a trapped charge gradient are assumed. Exponential dependence of pyroelectric current gives an activation energy of the order of 0.65 eV and is explained on the basis of new theory. Pyroelectric current of  $10^{-9}$  to  $10^{-10}$  A has been found in solvent-cast PVDF films.

## INTRODUCTION

Pyroelectric effect has been studied in many polymers.<sup>1-4</sup> Among these polymers, poly(vinylidene fluoride) (PVDF) has attracted special attention for its technological applications, such as switching devices,<sup>5</sup> radiation detectors,<sup>6</sup> electroacoustic transducers,<sup>7</sup> etc. PVDF exists in three crystalline forms,  $\alpha$ ,  $\beta$ , and  $\gamma$ . Todokoro et al.<sup>8</sup> have characterized these different forms, particularly by x-ray, NMR, infrared, and Raman studies. Both  $\alpha$  and  $\gamma$  forms possess monoclinic<sup>8</sup> configuration and are characterized respectively by 530  $\text{cm}^{-1}$  and 440  $\text{cm}^{-1}$  absorption bands. The  $\beta$  form is orthorhombic and appears with the absorption band 510  $\text{cm}^{-1}$  in perpendicular light. The molecule in the  $\beta$ -form crystal assumes a planar zigzag configuration,<sup>9</sup> and its dipole is oriented perpendicular to the chain axis. The dielectric studies<sup>10-12</sup> of PVDF reveal three relaxation regions,  $\alpha$ ,  $\beta$ , and  $\gamma$ , in the order of descending temperature.

The pyroelectric current in solvent-cast PVDF films, in which  $\beta$  crystals are preferentially oriented, has been observed to increase up to the melting point under short-circuit conditions. Many authors<sup>13-15</sup> studied simultaneously pyro- and piezoelectric effects in PVDF and have explained these effects on the basis of existence of the antisymmetric distribution of space charge embedded in the polymer. The antisymmetric distribution of space charge in polymer gives a qualitative view of the pyroelectric effect but does not provide any quantitative dependence of the pyroelectric current on temperature.

Pyroelectricity<sup>17,18</sup> has also been explained by measuring the relative contribution of the primary pyroelectric effect and the secondary pyroelectric effect to the total pyroelectric coefficient of PVDF. Primary pyroelectricity arises due to change in permanent dipolar polarization with temperature, whereas the change in sample dimensions with temperature causes secondary pyroelectricity. The results of these measurements have been described in terms of molecular and morphological structure<sup>19</sup> of PVDF.

Pyroelectricity has been reported for samples which are subjected to a strong DC electric field at elevated temperatures and then slowly cooled with the poling

field applied.<sup>15,16,20,21</sup> The application of the high electric field to PVDF film induces an electric polarization (Thermoelectret). Reversibility<sup>16,20-22</sup> of pyroelectric current in PVDF has been observed as a function of electric field. The pyroelectric current is reversible when the magnitude of pyroelectric current is the same during heating and cooling but with opposite sign.

In this paper a new model is proposed for pyroelectric effect, taking into account the hopping of trapped charge carriers over the potential barrier and the existence of a trapped charge gradient. Good agreement is found between theory and experiment for solvent-cast PVDF films.

## EXPERIMENTAL

In the present experiments, solvent-cast PVDF films were used to study the pyroelectric effect. Film was obtained by casting a dimethyl sulfoxide (DMSO) solution of PVDF on a glass plate at 60°C, as described elsewhere.<sup>23</sup> A film thickness of  $\sim 100\ \mu\text{m}$  was obtained, and samples 4 cm<sup>2</sup> in area were cut from the large sized film. The samples were provided with silver-evaporated electrodes on both sides to form a sandwich-type configuration. The sample was heated uniformly at a constant rate of 2°C/min between 20 and 170°C. The temperature was measured with the help of a chromel-constantan thermocouple. The Keithly 610C electrometer was employed to record the pyroelectric current as a function of temperature. A schematic representation of the experimental setup is shown in Figure 1.

## RESULTS

The pyroelectric current of PVDF film was measured as a function of temperature at a uniform heating rate of 2°C/min. In the first heating of the sample, the pyrocurrent shows a peak value at 90°C; it changes its polarity at 120°C, then increases continuously up to the melting point (curve a, Fig. 2). In the second heating cycle, no peak is observed, and current continuously increases after 70°C, as shown in curve b, Figure 2. The peak in the first heating cycle is considered to be due to the moisture content present in the sample, which is absent in the

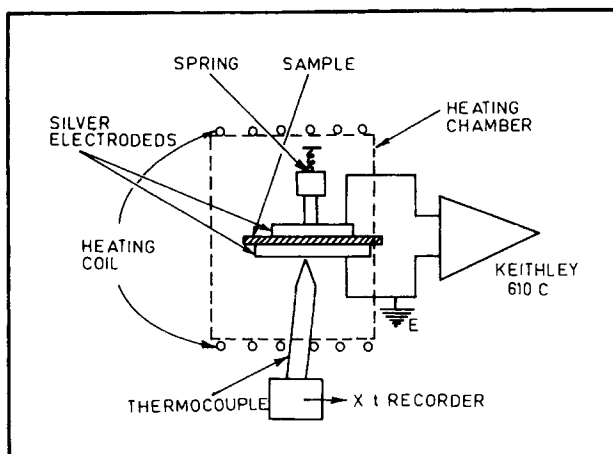


Fig. 1. Schematic representation of experimental setup for pyroelectric measurements.

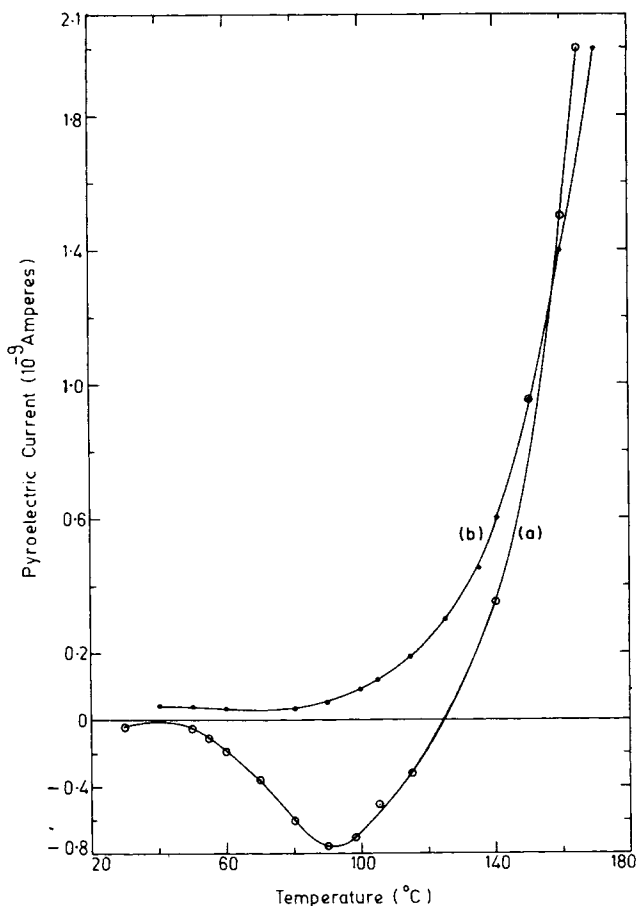


Fig. 2. Experimental plots of pyroelectric current vs. temperature for two successive heating cycles. Heating rate = 2°C/min. (○-○-○) 1st cycle; (●-●-●) 2nd cycle.

second heating. The moisture content in the virgin sample could be expected because of the internal polarization (PVDF is inherently polar) present in the film. In the successive cycles of heating, it was found that pyroelectric current follows the same curve (curve b, Fig. 2).

Figure 3 represents a semilog plot of pyroelectric current versus  $T^{-1}$ , which gives the exponential dependence of pyroelectric current on temperature. For  $T > 60^\circ\text{C}$ , an activation energy of 0.65 eV is obtained from this plot. The same order of activation energy was observed by Pfister et al.<sup>15</sup> in  $\beta$ -form PVDF film.

The pyroelectric current was also measured by applying different electrodes of Al and Cu, but no appreciable change in the behavior of pyroelectric current was observed. When two mica, Mylar, or Teflon sheets of 5- $\mu\text{m}$  thickness were inserted between the specimen and the electrodes, no current was detected. A similar type of experimental results on pyroelectric effect in PVDF has been observed by other workers.<sup>2,16</sup>

The true pyroelectric current<sup>16,22</sup> is known to be the same during heating and cooling but with opposite sign, i.e., pyroelectric current is reversible. Such re-

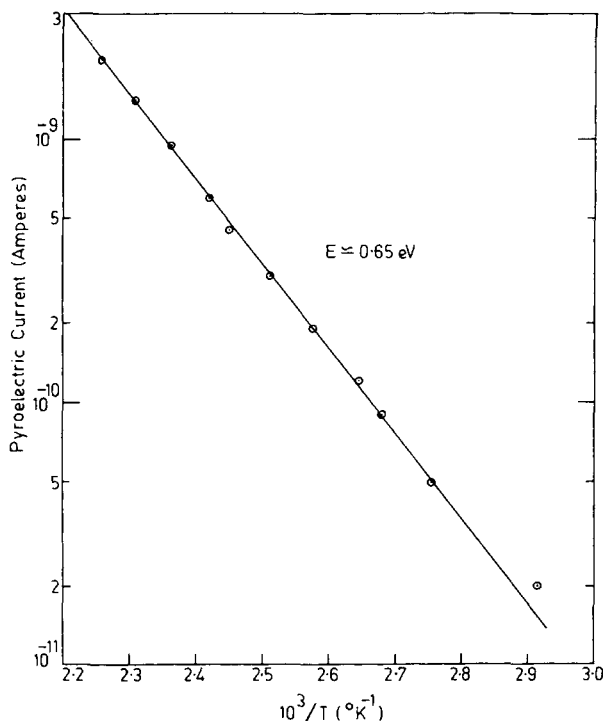


Fig. 3. Semilog plot of pyroelectric current vs. inverse of temperature.

versible pyroelectric currents<sup>16,22,24</sup> have been observed with  $\beta$ -form type PVDF and in specimens containing  $\beta$ -form and  $\alpha$ -form crystallites. Figure 4 shows the reversibility associated with the pyroelectric current measured in PVDF films. The reversible pyroelectric current in PVDF samples was observed by heating the short-circuited sample at a constant heating rate to a desired temperature and subsequent cooling to room temperature. In Figure 4 the pyroelectric current is almost reversible in nature; the small deviation from the reversibility may be caused by the small variation in the cooling rate. The reversible pyroelectric behavior has been attributed mainly to trapping effects.<sup>16</sup>

### PROPOSED MODEL AND DISCUSSION OF RESULTS

Pyroelectric current arises when the polymer sandwiched between two electrodes is uniformly heated. The origin of the pyroelectric effect has been a long controversy, and up till now no definite theory has evolved to explain the phenomenon. The importance of space charge has been proposed by several authors,<sup>13,14</sup> and pyroelectric effect has been attributed to the existence of trapped charges and their antisymmetrical distribution in the film. The pyroelectric current results from the drift of space charge to the electrodes under the image charge force when the capacitor is heated.<sup>15</sup> Though the antisymmetry distribution theory gives a qualitative explanation for pyroelectric current, it fails to provide the nature of the temperature dependence of the pyroelectric effect.

As the PVDF films contain both amorphous and crystalline regions,<sup>16,19</sup> the

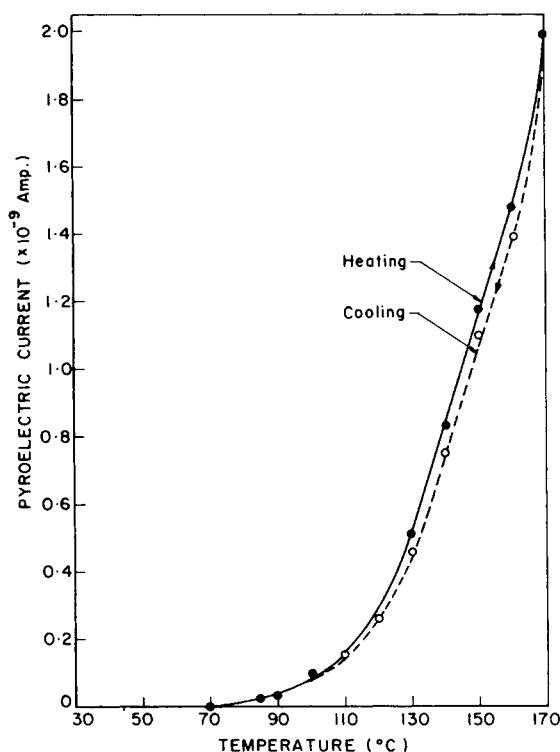


Fig. 4. Typical reversible pyroelectric current in PVDF. Heating/cooling rate =  $2^{\circ}\text{C}/\text{min}$ .

pyroelectricity can be thought to arise in terms of a hopping mechanism. Hopping of the embedded trap charges takes place over the potential barrier, and the potential barrier height is decided by the active trap species participating in the pyroelectric effect. The net flow of the charge carriers (held in traps) in a particular direction will depend upon the direction of internal polarization and the orientation of the paired potential barrier wells. The amount of net charges hopping in that direction will depend upon the strength of internal polarization and temperature.

Polymeric films are usually macroscopically isotropic. The anisotropy may be introduced in the plane of the film after stretching, but they are still isotropic in the thickness direction.<sup>2</sup> The solution-cast PVDF films can be assumed to be isotropic in the thickness direction ( $x$  axis). The distribution of trapped space charge, however, may be inhomogeneously distributed in film plane and in the  $x$  axis. Since pyroelectric current is a consequence of the uniform heating of the polymer film, the pyroelectric current can be thought to arise from the thermally activated hopping of the nonuniformly distributed trapped space charge over the potential energy barrier.

In view of the above physical picture, the present quantitative theory has been developed, using the following assumptions:

- (1) Internal polarization exists in the sample, which gives rise to the internal field  $E_{\text{in}}$ ;
- (2) Nonuniform distribution of trapped space charge exists, i.e., space charge density  $\rho_t$  is a function of position ( $d\rho_t/dx \neq 0$ ); and
- (3) Hopping of the trapped charge carriers over the potential barrier.

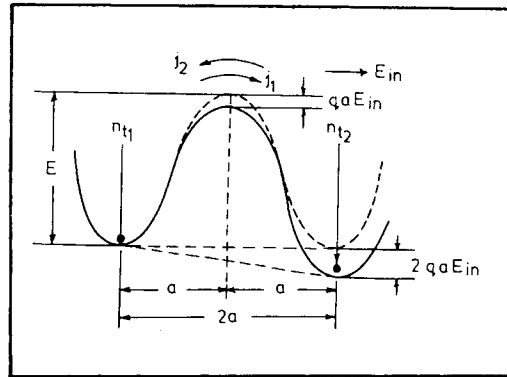


Fig. 5. Potential barrier model for pyroelectric effect.

The physical picture of hopping over the potential barrier is shown in Figure 5. The symmetric barrier denoted by the dotted line represents such a barrier in zero field, whereas the asymmetric barrier denoted by the solid line represents the field-modified barrier (Fig. 5). An electric field ( $E_{in}$ ) due to internal polarization lowers a barrier  $E$  for charge carrier motion in the forward direction by an amount  $qaE_{in}$ , where  $q$  is the elementary charge. When the temperature is increased, the probability for the charge carrier to surmount the barrier increases, and hence the net charge flow over the barrier in one direction increases, which gives rise to pyroelectric current. The hopping frequencies for the zero field and field-modified barrier are, respectively,

$$\nu \exp [-(E - qaE_{in}/kT)] \quad (1a)$$

$$\nu \exp [-(E + qaE_{in}/kT)] \quad (1b)$$

where  $\nu$  is the attempt-to-escape frequency.

The net number  $j$  of charges per unit area surmounting the barrier per unit time is

$$j = j_1 - j_2 = n_{t1}\nu \exp [-E - qaE_{in}/kT] - n_{t2}\nu \exp [-(E + qaE_{in}/kT)] \quad (2)$$

The value  $n_{t1}$  denotes the trapped charges per unit area in a planar slice normal to the hopping direction in potential well 1,  $n_{t2}$  denotes the corresponding number of the carriers present in potential well 2, and  $2a$  is the separation between two potential wells. This corresponds to the current in the medium. The following cases can be derived from eq. (2) depending upon the concentration gradient and the internal electric field  $E_{in}$ :

- (1) When  $n_{t1} - n_{t2} = 0$  (zero concentration gradient),

$$j \simeq 2n_{t1}\nu \exp (-E/kT) \sinh (qaE_{in}/kT) \quad (3)$$

- (2) When  $E_{in}$  is very large, i.e.,  $|E_{in}| \gg |kT/qa|$ ,

$$j \simeq n_{t1}\nu \exp (+E/kT) \exp (qaE_{in}/kT) \quad (4)$$

- (3) When  $E_{in}$  is intermediate or low,  $|E_{in}| \gg |kT/qa|$ ,

$$j = (2qaE_{in}n_{t1}/kT)\nu \exp (-E/kT) \quad (5)$$

- (4) When concentration gradient is nonzero, ( $n_{t1} - n_{t2} \neq 0$ ), and  $E_{in}$  is very low,

$$j = (n_{t1} - n_{t2})\nu \exp(-E/kT) \quad (6)$$

The term  $q[(n_{t1} - n_{t2})/2a]$  represents the average bulk concentration of trapped in the potential wells. Thus, we can write

$$q \frac{dN_t(x)}{dx} = \frac{d\rho_t(x)}{dx} = q \frac{(n_{t1} - n_{t2})/2a}{2a} \quad (7)$$

$$j = (dN_t(x)/dx)4a^2\nu \exp(-E/kT) \quad (8)$$

where  $N_t$  is the number of trapping charge per unit volume. The electric current density  $J$  due to charge carrier current  $j$  is

$$J = qj = (d\rho_t(x)/dx)4a^2\nu \exp(-E/kT) \quad (9)$$

This represents the thermally activated hopping produced by the concentration gradient of trapped charges in a very weak field  $E_{in}$ . Statistically there will be net motion of the trapped charges away from the region where the concentration is larger to regions where the concentration is smaller. This net motion of charges will depend upon the temperature.

Equation (9) can be solved for a uniform rate of rise of temperature. The variation of the current density  $J$  is given by the expression

$$J = \frac{d\rho_{t0}(x)}{dx} 4a^2\nu \exp\left(-\frac{E}{kT}\right) \exp\left[-\int_{T_0}^T \frac{4a^2\nu \exp(-E/kT)}{\beta} dT\right] \quad (10)$$

where  $\rho_{t0}(x)$  is the density of trapped charge at initial temperature  $T = T_0$  and  $\beta$  is the heating rate ( $T = T_0 + \beta t$ ). For the temperature range used in the present experiments,  $E \gg kT$ ; and for moderate heating rate, eq. (10) can be approximated as

$$J \simeq (d\rho_{t0}(x)/dx) 4a^2\nu \exp(-E/kT) \quad (11)$$

For single potential barrier approximation, we consider the interfaces of the film to be at the potential minima located at  $x = 0, x = L$ , respectively. Then eq. (11) will give the current in the circuit when the film is heated. Equation (11) can be employed to account for the pyroelectric effect under very weak field condition. Since for the pyroelectric current of  $\sim 10^{-9}$ – $10^{-10}$  A, the voltage developed across the sample when heated never exceeds  $3 \times 10^{-4}$  V; therefore, eq. (11) can be used to explain the pyroelectric effect. According to eq. (11), the pyroelectric current should increase exponentially with temperature, which has been found experimentally as shown in Figure 3 and by others.<sup>16</sup> The activation energy evaluated from Figure 3 is  $\sim 0.65$  eV, which provides the barrier height. It is interesting to estimate numerically the order of magnitude of pyroelectric current if the concentration gradient of charges over the potential well is  $dN_{t0}/dx \simeq 10^{12}$  cm<sup>-2</sup>,  $E = 0.65$  eV,  $T = 400$  K,  $\nu = 10^{12}$ /sec, and  $q = 1.6 \times 10^{-19}$  C,  $a \sim 10^{-4}$  cm, and area of the sample  $\sim 4$  cm<sup>2</sup>. The pyroelectric current is then estimated to be  $10^{-10}$  A. This order of current is usually observed in pyroelectric materials.

Good estimation of the pyroelectric current from Eq. (11) needs accurate values of parameters  $a$ ,  $\nu$ , and  $dN_t/dx$ . These values can be determined from other types of experiments. In the present work, we have assumed the existence of one potential well only, and this theory can be modified taking into account the hopping over series of such barriers. Such calculations may be complicated but

are expected to give a more accurate account for PE. Work in this direction is in progress.

The authors are grateful to Prof. P. K. C. Pillai, Department of Physics, I.I.T. Delhi, for his encouragement and fruitful discussion. One of the authors, Mrs. T. K., is thankful to C.S.I.R. (India) for financial support.

### References

1. M. L. Miller and J. R. Murray, *J. Polym. Sci. Part A-2*, **4**, 69 (1966).
2. T. Fukurawa, T. Uematsu, K. Asakawa, and Y. Wada, *J. Appl. Polym. Sci.*, **12**, 2675 (1968).
3. L. M. Baxt and M. M. Perlman, *Electrets and Related Electrostatic Charge Storage Phenomena*, The Electrochemical Society, New York, 1968.
4. F. Mopsik and M. G. Broadhurst, *J. Appl. Phys.*, **46**, 4204 (1975).
5. R. J. Phelan, Jr., R. L. Peterson, G. A. Himilton, and G. W. Day, Third International Meeting on Ferroelectricity, September 10, 1973, Edinburgh, Scotland.
6. R. J. Phelan, Jr., and A. R. Cock, *Appl. Opt.*, **12**, 2494 (1973).
7. N. Murayama, K. Nakamura, H. Obara, and M. Segawa, *Ultrasonics*, January 1976, pp. 15-23.
8. Todokoro et al., *Macromolecules*, **8**, 100 (1975).
9. M. Latour, *Polymer*, **18**, 278 (1977).
10. J. B. Lando, H. G. Olf, and A. Peterlin, *J. Polym. Sci. Part A-1*, **4**, 941 (1966).
11. A. Peterlin and J. H. Elwell, *J. Mater. Sci.*, **2**, 1 (1967).
12. T. Takamatsu and E. Fukeda, *Polym. J. Jpn.* **1**, 101 (1970).
13. K. Nakamura and Y. Wada, *J. Polym. Sci. Part A-2*, **9**, 161 (1971).
14. T. Furukawa, Y. Wematsu, K. Asakawa, and Y. Wada, *J. Appl. Polym. Sci.*, **12**, 2675 (1968).
15. N. Murayama and H. Hashizume, *J. Polym. Sci.*, **14**, 989 (1976).
16. G. Pfister, M. Abkowitz, and R. G. Crystal, *J. Appl. Phys.*, **44**, 2064 (1973).
17. R. G. Kepler and R. A. Andersons, *J. Appl. Phys.*, **43**, 4490 (1978).
18. R. G. Kepler and R. A. Andersons, *J. Appl. Phys.*, **49**, 4918 (1978).
19. M. G. Broadhurst, G. T. Davis, J. E. McKinney, and R. E. Collins, *J. Appl. Phys.*, **49**, 4992 (1978).
20. G. T. Davis, J. E. McKinney, M. G. Broadhurst, and S. C. Roth, *J. Appl. Phys.*, **49**, 4998 (1978).
21. M. Abkowitz and G. Pfister, *J. Appl. Phys.*, **46**, 2559 (1975).
22. D. K. Das Gupta, *J. Appl. Phys.*, **50**, 561 (1979).
23. M. Asahina et al., 18th Polymer Symposium, October 1967, Tokyo, Preprints, p. 449.
24. H. Bukard and G. Pfister, *J. Appl. Phys.*, **45**, 3360 (1974).

Received April 9, 1979

Revised September 27, 1979